

Infrared Quantum Cascade Laser

W. Schrenk, N. Finger, S. Gianordoli, L. Hvozdar, E. Gornik,
and G. Strasser

Institut für Festkörperelektronik, Technische Universität Wien
Floragasse 7, 1040 Wien, Austria

We report on quantum cascade lasers in the AlGaAs material system grown on GaAs. The emission wavelength is in the range of $\lambda \sim 9.5 - 13 \mu\text{m}$. Both, first and second order distributed feedback laser have been fabricated. A metallized surface-relief grating is used for feedback to achieve single-mode emission. The emission wavelength is continuously tunable with the heat sink temperature. The second order distributed feedback lasers are efficient surface emitters with low beam divergence. Further, continuous wave operation at cryogenic temperatures has been achieved for a chirped superlattice active region.

1. Introduction

A quantum cascade laser (QCL) is a semiconductor laser involving only one type of carrier and which is based on two fundamental phenomena of quantum mechanics, namely, tunneling and quantum confinement. In conventional semiconductor diode lasers (as used, e.g., in compact disk players), the light originates from the recombination of electrons and holes, and the emission wavelength is determined by the bandgap. However, in QCLs the light generation is based on intersubband transitions within the conduction band (or valence band). So far, QCLs are demonstrated only in two material systems, the InGaAs/InAlAs material system grown on InP [1] and the AlGaAs/GaAs grown on GaAs [2]. Spontaneous emission from quantum cascade structures has been achieved in some other materials [3], [4]. Recently, room temperature operation of AlGaAs based QCL [5] has been demonstrated for Fabry Perot lasers, which is an important step towards commercial applications. Up to this, room temperature operation was a privilege for QCL grown on InP. Continuous wave operation of QCL is so far restricted to low temperatures [6], also for QCL grown on InP [7] – [9]. However, for absorption measurements like gas sensing, single mode lasers are favored. Therefore, distributed feedback (DFB) QCL [10] – [13] have been realized soon after the invention of QCLs. Some demonstration of infrared spectroscopy of gases [14] – [16] (single- or multiple pass absorption), liquids [17] or photoacoustic spectroscopy [18] show the potential for commercial applications. In this letter, we report on distributed feedback quantum cascade lasers in the AlGaAs material system grown on GaAs.

2. Experimental

The energy band diagram (conduction band) of a typical QCL is shown in Fig. 1. The electrons are injected into the upper laser level 3 by an electron funnel (injector). Inversion is achieved by fast depopulation of level 2 by LO-phonon emission (lifetime ~ 0.3 ps). Therefore the energy spacing of level 2 and level 1 is designed close to the LO-

phonon energy of GaAs (36 meV). The lifetime of the upper laser level is in the range of 2 ps, allowing fast direct modulation.

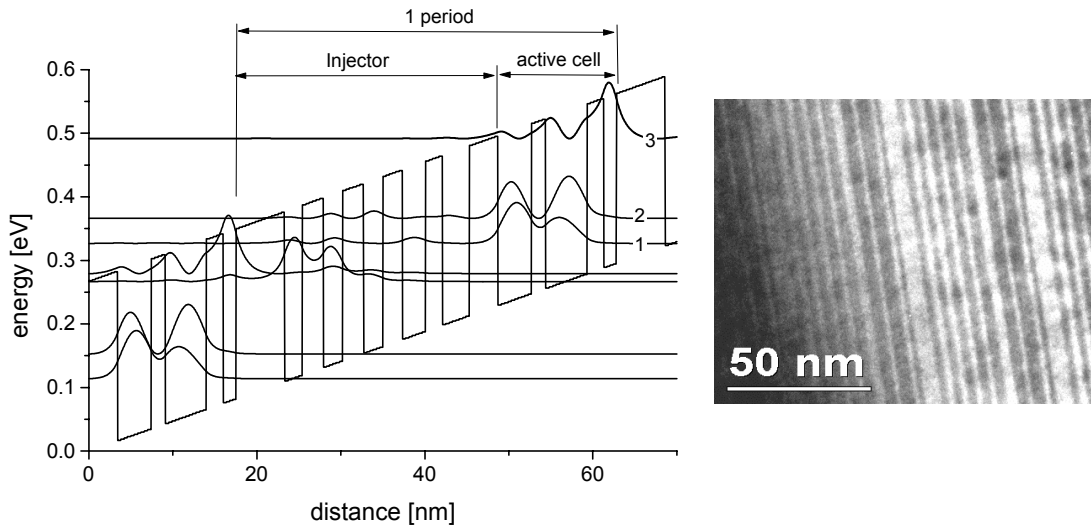


Fig. 1: Left: Energy band structure and moduli square of the most relevant wave functions of a QCL. The laser transition is the transition 3–2, and the energy separation of the level 2 and 1 is close to the LO-phonon energy. Right: Transmission electron microscope picture of a MBE grown QCL.

We have used $\text{Al}_{0.33}\text{Ga}_{0.67}\text{As}$ or AlAs as barrier material and GaAs or $\text{In}_{0.04}\text{Ga}_{0.96}\text{As}$ as well material for our lasers. The active cell is formed by three quantum wells or by a chirped superlattice. The superlattice is chirped in order to get flat minibands for the design field. The conduction band discontinuity and the energy of the upper laser level determines the leakage current into the continuum, which restricted the very first $\text{Al}_{0.33}\text{Ga}_{0.67}\text{As}/\text{GaAs}$ based QCL to low operation temperatures as the upper laser level is close to the barrier energy (Fig. 1). In the first structures we used $\text{Al}_{0.33}\text{Ga}_{0.67}\text{As}$ as barrier material, where the X-valley is higher in energy than the Γ -valley in order to get rid of multi valley effects as the crossover from a direct to an indirect semiconductor occurs for $\text{Al}_x\text{Ga}_{1-x}\text{As}$ at $x \sim 0.45$. We have also investigated InGaAs as well material, which increased the band offset in respect to $\text{Al}_{0.33}\text{Ga}_{0.67}\text{As}$ [19]. The lattice mismatch of $\text{In}_x\text{Ga}_{1-x}\text{As}$ grown on GaAs allowed only low In contents. Then we used AlAs as barrier material, where the overall Al concentration is small and the AlAs layers are very thin (down to 2 monolayers) so that the electrons remain around the Γ -valley. In this case, the lowest energy levels for the X-valleys (GaAs and AlAs) are higher than for the Γ -valley. An AlAs/GaAs chirped superlattice laser material showed the first time continuous wave operation for GaAs based QCL.

Our laser material is grown by solid source molecular beam epitaxy on n-doped GaAs (100). A double plasmon enhanced waveguide is used for all lasers. 30 to 40 periods of active cell/injector are cascaded and embedded into low doped GaAs (Si , $4 \times 10^{16} \text{ cm}^{-3}$, $d \sim 3.5 \mu\text{m}$) layers, forming the low loss waveguide core. The cladding layers are formed by highly doped GaAs (Si , $4 \times 10^{18} \text{ cm}^{-3}$, $d \sim 1.0 \mu\text{m}$).

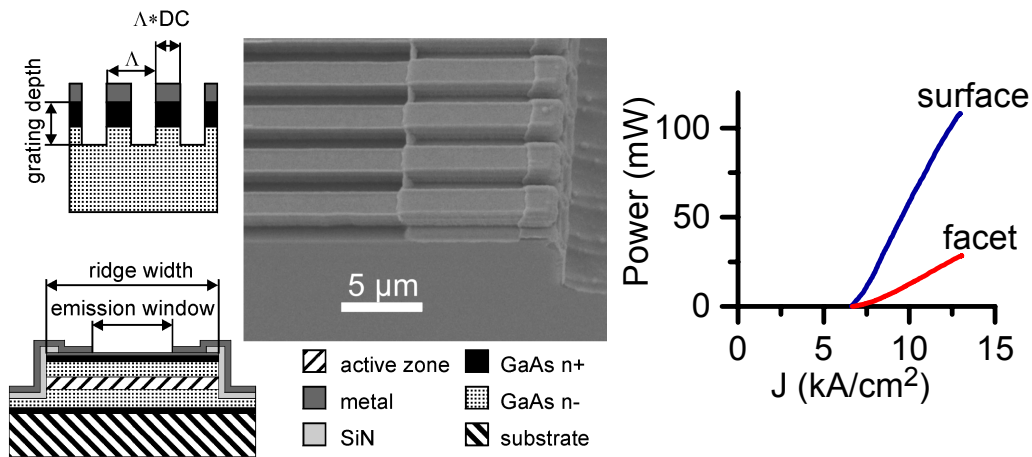


Fig. 2: Left: Schematic cross section of the grating region and the ridge waveguide, and a SEM picture of a fabricated laser. Λ denotes the grating period and DC is the duty cycle of the grating. Right: Emitted power via surface and one facet for a 2.99 mm long and 45 μm wide laser in pulsed mode operation (100 ns, 5 kHz).

We have fabricated DFB laser from several laser materials [6], [13], [20]. A metallized surface relief grating is used for feedback, resulting in a large contact area and avoiding the need of regrowth. The coupling coefficients and losses are calculated based on Floquet Bloch analysis [21]. The Floquet Bloch fields are rigorously calculated at resonance and a connection to the coupled mode theory is made by a perturbation method, as the optical intensity in the grating region is small. In the case of first order DFB laser the whole grating is covered with metal whereas in the case of the second order DFB laser only the grating peaks (Fig. 2) are covered with metal allowing efficient transmission of the TM polarized light through the metal stripe structure. We have fabricated ridge waveguides where we etched through the active region. The lateral light confinement is almost unity whereas the vertical light confinement by the plasmon enhanced waveguide (in growth direction) is in the range of 0.3 – 0.5.

The absolute average power is measured with a slow thermopile detector. The pulse peak power in pulsed mode operation (pulse length 100 ns) is in the several 100 mW range (Fig. 2). Spectral measurements were performed with a Fourier transform infrared (FTIR) spectrometer equipped with a mercury-cadmium-telluride (MCT) detector. As the current heats the active region, the emission wavelength is shifted to longer wavelengths during a pulse causing a broadening of the emission in pulsed mode operation. The current heating can be neglected for short pulses and low pulse repetition rates. The emission wavelength is in this case only a function of the heat sink temperature. The emission wavelength shifts according to the Bragg wavelength and the temperature dependence of the refractive index at a rate of $(d\lambda/dT)/\lambda \sim 1 \times 10^{-5}/\text{K}$ (Fig. 3). In continuous wave operation the emission tunes with the current (Fig. 3) corresponding to temperature within the laser cavity.

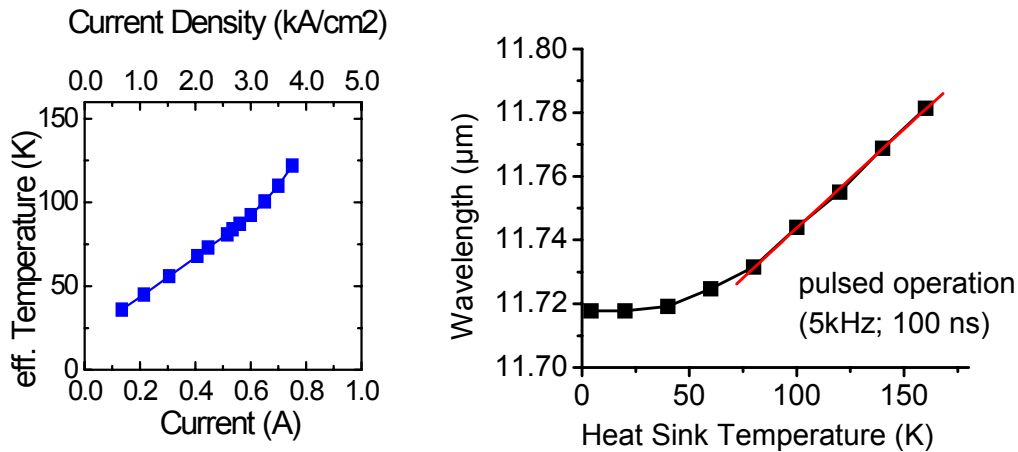


Fig. 3: Left: Effective temperature in the laser cavity for continuous wave operation as obtained from the emission wavelength (heat sink temperature 4.2 K). Right: Emission wavelength in pulsed mode operation (100 ns, 5 kHz) as a function of the heat sink temperature for the same laser.

3. Conclusion

In conclusion, we have achieved single mode emission in the mid-infrared from quantum cascade lasers grown on GaAs. The emission wavelength is continuously tunable by the temperature. We have developed an analysis which allows the accurate prediction of the coupling coefficient and the losses of the waveguide grating structure, including the surface emission of second order DFB lasers. Further, continuous wave operation at low temperatures has been achieved for a DFB laser emitting at 11.7 μm .

Acknowledgements

This work was partly supported by the European Community by the research projects SUPERSMILE IST-1999-1493 and UNISEL (Brite Euram III) BE97-4072 and the FWF Austria.

References

- [1] J. Faist, F. Capasso, D. L. Sivco, C. Sirtori, A. L. Hutchinson, and A. Y. Cho, "Quantum Cascade Laser", *Science* **264**, 1994, pp. 553.
- [2] C. Sirtori, P. Kruck, S. Barbieri, P. Collot, J. Nagle, M. Beck, J. Faist, and U. Oesterle, "GaAs/Al_xGa_{1-x}As quantum cascade lasers", *Appl. Phys. Lett.* **73**, 1998, pp. 3486.
- [3] G. Dehlinger, L. Diehl, U. Gennser, H. Sigg, J. Faist, K. Ensslin, D. Grützmacher, and E. Müller, "Intersubband Electroluminescence from Silicon-Based Quantum Cascade Structures", *Science* **290**, 2277 (2000).

- [4] C. Becker, I. Prevot, X. Marcadet, B. Vinter, and C. Sirtori, "InAs/AlSb quantum-cascade light-emitting devices in the 3-5 μm wavelength region", *Appl. Phys. Lett.* **78**, 2001, pp. 1029.
- [5] H. Page, C. Becker, A. Robertson, G. Glastre, V. Ortiz, and C. Sirtori, "300 K Operation of a GaAs based Quantum Cascade Laser at $\lambda = 9 \mu\text{m}$ ", *Appl. Phys. Lett.*, in print.
- [6] W. Schrenk, N. Finger, S. Gianordoli, E. Gornik, and G. Strasser, "Continuous-wave operation of distributed feedback AlAs/GaAs superlattice quantum-cascade lasers", *Appl. Phys. Lett.* **77**, 2000, pp. 3328.
- [7] J. Faist, F. Capasso, C. Sirtori, D. L. Sivco, A. L. Hutchinson, and A. Y. Cho, "Continuous wave operation of a vertical transition quantum cascade laser above $T=80 \text{ K}$ ", *Appl. Phys. Lett.* **67**, 1995, pp. 3057.
- [8] R. Köhler, C. Gmachl, A. Tredicucci, F. Capasso, D. L. Sivco, S. N. G. Chu, and A. Y. Cho, "Single-Mode Tunable Quantum Cascade Lasers in the Spectral Range of the CO_2 Laser at $\lambda = 9.5\text{-}10.5 \mu\text{m}$ ", *Appl. Phys. Lett.* **76**, 2000, pp. 1092.
- [9] A. Tahraoui, A. Matlis, S. Slivken, J. Diaz, and M. Razeghi, "High-performance quantum cascade lasers ($\lambda \sim 11 \mu\text{m}$) operating at high temperature ($T \geq 425 \text{ K}$)", *Appl. Phys. Lett.* **78**, 2001, pp. 416.
- [10] C. Gmachl, J. Faist, J. N. Baillargeon, F. Capasso, C. Sirtori, D. L. Sivco, S. N. G. Chu, and A. Y. Cho, "Complex-Coupled Quantum Cascade Distributed-Feedback Laser", *IEEE Photonics Technol. Lett.* **9**, 1997, pp. 1090.
- [11] J. Faist, C. Gmachl, F. Capasso, C. Sirtori, D. L. Sivco, J. N. Baillargeon, and A. Y. Cho, "Distributed feedback quantum cascade lasers", *Appl. Phys. Lett.* **70**, 1997, pp. 2670.
- [12] D. Hofstetter, M. Beck, T. Aellen, and J. Faist, "High-temperature operation of distributed feedback quantum-cascade lasers at $5.3 \mu\text{m}$ ", *Appl. Phys. Lett.* **78**, 2001, pp. 396 – 398.
- [13] W. Schrenk, N. Finger, S. Gianordoli, L. Hvozdar, G. Strasser, and E. Gornik, "GaAs/AlGaAs distributed feedback quantum cascade lasers", *Appl. Phys. Lett.* **76**, 2000, pp. 253.
- [14] C. R. Webster, G. J. Flesch, D. C. Scott, J. E. Swanson, R. D. May, W. S. Woodward, C. Gmachl, F. Capasso, D. L. Sivco, J. N. Baillargeon, A. L. Hutchinson, and A. Y. Cho, "Quantum-cascade laser measurements of stratospheric methane and nitrous oxide" *Appl. Optics* **40**, 2001, pp. 321.
- [15] L. Hvozdar, S. Gianordoli, G. Strasser, W. Schrenk, K. Unterrainer, E. Gornik, C. S. S. S. Murthy, M. Kraft, V. Pustogow, B. Mizaikoff, A. Inberg, N. Croitoru, "Spectroscopy in the Gas Phase with GaAs/AlGaAs Quantum-Cascade Lasers", *Appl. Optics* **39**, 2000, pp. 6926 – 6930.
- [16] A. A. Kosterev, F. K. Tittel, C. Gmachl, F. Capasso, D. L. Sivco, J. N. Baillargeon, A. L. Hutchinson, A. Y. Cho, "Trace-gas detection in ambient air with an thermoelectrically cooled, pulsed quantum-cascade distributed feedback laser" *Appl. Optics* **39**, 2000, pp. 6866 – 6872.

- [17] B. Lendl, J. Frank, R. Schindler, A. Müller, M. Beck, and J. Faist, "Mid-Infrared Quantum Cascade Lasers for Flow Injection Analysis", *Analytical Chemistry* **72**, 2000, pp. 1645 – 1648.
- [18] B. A. Paldus, T. G. Spence, R. N. Zare, J. Oomens, F. J. M. Harren, D. H. Parker, C. Gmachl, F. Capasso, D. L. Sivco, J. N. Baillargeon, A. L. Hutchinson, A. Y. Cho, " Photoacoustic spectroscopy using quantum-cascade lasers ", *Optics Lett.* **24**, 1999, pp. 178 – 180.
- [19] S. Gianordoli, W. Schrenk, L. Hvozdar, N. Finger, G. Strasser, and E. Gornik, "Strained InGaAs/AlGaAs/GaAs-quantum cascade lasers", *Appl. Phys. Lett.* **76**, 2000, pp. 3361.
- [20] W. Schrenk, N. Finger, S. Gianordoli, L. Hvozdar, G. Strasser, and E. Gornik, "Surface-emitting distributed feedback quantum-cascade lasers", *Appl. Phys. Lett.* **77**, 2000, pp. 2086.
- [21] N. Finger, W. Schrenk, and E. Gornik, "Analysis of TM-Polarized DFB Laser Structures with Metal Surface Gratings", *IEEE J. Quant. Electron.* **36**, 2000, pp. 773.